JOURNAL OF SANDWICH STRUCTURES & MATERIALS

Original Article

Journal of Sandwich Structures and Materials
0(00) 1–16

DOI: 10.1177/1099636216650989
jsm.sagepub.com
SAGE

Nanowire reinforcement of woven composites for enhancing interlaminar fracture toughness

AG Castellanos, MS Islam, MAI Shuvo, Y Lin and P Prabhakar

Abstract

A novel technique to improve the Mode I and Mode II interlaminar fracture toughness of woven carbon-fiber polymer matrix composite face sheets using zinc oxide nanowires is proposed. Zinc oxide nanowires are directionally synthesized on dry carbon fabrics that are used to manufacture the laminate. The influence of zinc oxide nanowires on interlaminar fracture toughness is compared against regular interfaces using double cantilever beam and end-notched flexure tests to provide fracture toughness values. A significant improvement in the Mode I and Mode II interlaminar fracture toughness values is observed with zinc oxide nanowires. Therefore, zinc oxide nanowire interlaminar reinforcement has been proven to enhance the interlaminar fracture toughness of textile composites.

Keywords

Textile composites, fracture toughness, zinc oxide nanowires, interface, delamination

Introduction

Composite materials have become an attractive replacement for conventional materials, such as steel or aluminum, to improve performance and reduce the weight of high-performance structures [1]. Their use has been successfully integrated into aerospace vehicles, wind energy turbine blades, rockets, marine structures, and automobiles [2], owing to their tailorable mechanical properties and high

Department of Mechanical Engineering, University of Texas at El Paso, USA

Corresponding author:
Pavana Prabhakar, Department of Mechanical Engineering, University of Texas at El Paso, El Paso, TX 79968, USA.
Email: pprabhakar@utep.edu

specific stiffness, strength-to-weight ratios, corrosion, and fatigue resistance [3,4]. In particular, sandwich composites are used in ship hulls because of their high bending stiffness. Sandwich composites consist of a core sandwiched between face sheets. To improve the damage resistance and durability of sandwich composites, it is essential to improve the properties of both the face sheets and the core. In this study, the focus is on improving the interlaminar fracture toughness of carbon-fiber-reinforced face sheet composites.

Carbon-fiber-reinforced woven composites consist of layers of woven carbon fabric in a polymer matrix. Although the in-plane stiffness and strength of these composites are high, the resin-rich region interlaminar region between the carbon-fiber layers of the composite is susceptible to damage and can result in premature failure of the composite [5,6]. The life of a composite structure depends on its response to different failure mechanisms, such as delamination or interlaminar fracture, matrix cracking, matrix-fiber debonding, fiber breaking, and fiber pullout [7,8].

Delamination or interlaminar fracture is one of the most common failure mechanisms in composites [7]. Delamination can occur as a result of manufacturing defects, such as bad lay-up, cracks between layers, weaker matrix phase, etc. or in service, owing to interlaminar stresses, impact, static overload and fatigue [9–13]. This often results in a reduction in stiffness and strength of the composites, leading to global failure of the composite structure. Therefore, in this study, interlaminar fracture toughness is investigated, to establish the damage resistance and tolerance of a composite structure. Interlaminar fracture toughness is the amount of energy required to create fracture surfaces under three fracture modes: Mode I (opening mode), Mode II (sliding shear mode) and Mode III (scissoring shear mode) [9,14]. The focus of this study is on enhancing the pure Mode I and Mode II interlaminar fracture of carbon-fiber woven textile composites.

Different through-thickness reinforcements have been studied by earlier researchers, including stitching, weaving, braiding [13], and *z*-pins [15], to improve the interlaminar fracture toughness of composites. Although an increase in through-thickness response was observed, these methods have been shown to decrease the in-plane properties, owing to reduction in the in-plane volume fraction, damaging the reinforcing fibers or creating large resin pockets [13,16]. Another method is the application of nanofiber carbon nanotubes on the surface of the dry fabric by chemical vapor deposition. However, carbon nanotubes do not distribute uniformly, tending to create bundles and branches [6,17]. Further, the techniques that currently exist to disperse the carbon nanotubes tend to damage the carbon fiber [6,18,19]. Moreover, several studies reported a decrease in the tensile strength of the fibers after carbon nanotubes had been grown on them [16]. Qian et al. [20] reported a decrease in fiber tensile properties by nearly 55%. To prevent damage in the fiber due to high growth temperature and reduction of in-plane properties, a low-temperature solution-based fabrication of ZnO nanowires as interlaminar reinforcements was studied.

According to Kong et al., [21] different types of nanowire can enhance interfacial mechanical properties; however, ZnO nanowires are expected to be less prone to

impact damage. Recent results from Hwang et al. [22] have shown that vertically aligned ZnO nanowires lead to approximately 23 times higher energy absorption and 11 times higher peak load than pristine composites. ZnO nanowires also have piezoelectric and semiconducting properties, which make them well suitable for solar cells [23], dynamic sensors [24], and energy harvesting materials [25]. A recent study by Lin et al. [26] has shown that ZnO nanowires improve the interfacial shear strength of the individual carbon fibers by 113% and the laminar shear strength and modulus by 37.8% and 38.8%, respectively. In this study, the influence of ZnO nanowires on the Mode I and Mode II interlaminar fracture toughness of carbon-fiber woven composites was investigated. To our knowledge, this is the first time that ZnO nanowires have been used as a means to improve the interlaminar fracture toughness of woven composites.

Carbon-fiber woven composites were primarily studied. ZnO nanowires were synthesized on dry fabric, and the composites were manufactured using vacuum-assisted resin transfer molding (VARTM). The interlaminar Mode I and Mode II fracture toughness with and without nanowires were compared using double cantilever beam and end-notched flexure tests, respectively. A significant improvement in Mode I and Mode II fracture toughness of the interfaces was observed as a result of ZnO nanowire reinforcement.

The paper is organized in the following sections: a brief description of the VARTM process for composite manufacturing and ZnO nanowire synthesis on fabrics is given next, followed by the test methods used to determine Mode I and Mode II fracture toughness values. Finally, a comparison of interlaminar fracture toughness values between laminates with and without ZnO nanowire reinforcement is provided before conclusions are made.

Manufacturing

The VARTM process for composite manufacturing

The VARTM process [27] was used to manufacture woven composites with and without ZnO nanowires. Laminates were fabricated by placing layers of dry carbon fabric in a mold with flow media, e.g. breather or nylon peel ply, as shown in Figure 1(a). This was followed by enclosing the mold in a vacuum bag (see Figure 1(b)) and drawing it into a vacuum, to aid infiltration of the resin [27]. Laminates were manufactured with 8 layers of dry fabric for Mode I tests and 20 layers for Mode II tests. Dry plain-weave fabrics were used as reinforcement with vinyl ester resin and methyl ethyl ketone peroxide hardener as matrix material. The resin was catalyzed with 1.25% methyl ethyl ketone peroxide (by weight) and mixed thoroughly for one minute, as recommended by the manufacturer. All the specimens (with and without ZnO nanowires) for the double cantilever beam and end-notched flexure tests were fabricated as single laminates, as shown in Figure 1(c) and (d) to ensure that the curing conditions were identical. A Teflon sheet of 0.05 mm (0.002 in) thickness was placed between the 4th and the 5th layers

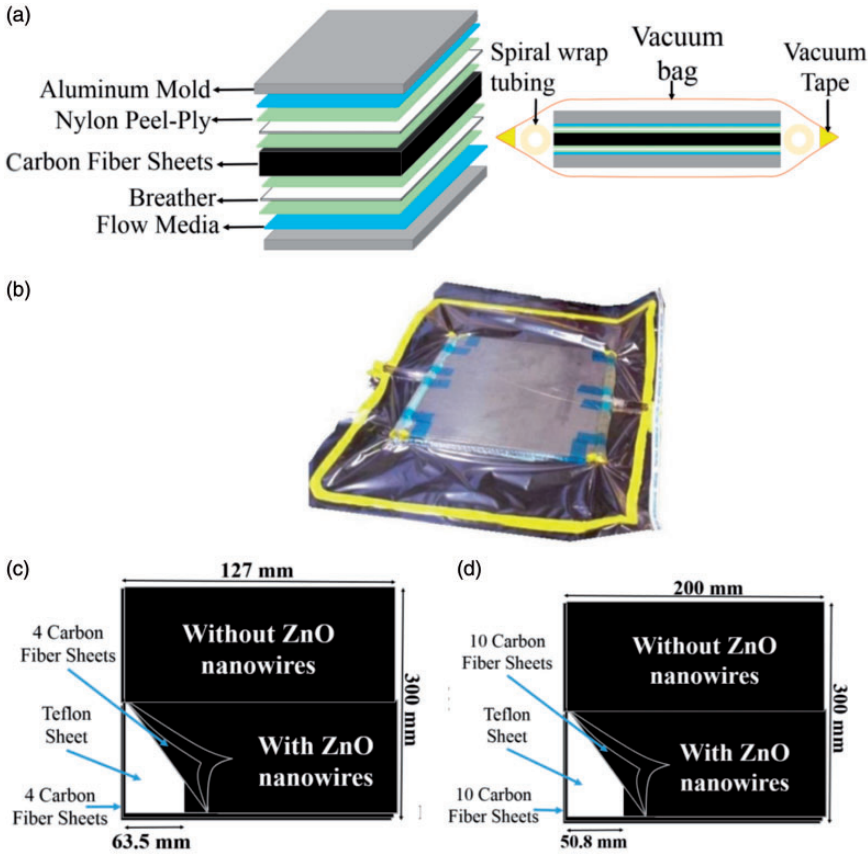

Figure 1. (a) VARTM configuration for the 2D carbon woven composite; (b) Laminate preparation in progress using VARTM process; (c) Teflon sheet insert to simulate a crack for double cantilever beam sample; (d) Teflon sheet insert to simulate a crack for end-notched flexure sample.

to create a pre-crack for the double cantilever beam test samples (Figure 1(c)), and between the 10th and 11th layers for the end-notched flexure test samples (Figure 1(d)). Furthermore, ZnO nanowires were synthesized on the surfaces of the 4th and the 5th layers for Mode I tests and on the surfaces of the 10th and 11th layers for Mode II tests, thereby reinforcing the fracturing interface of the double cantilever beam and end-notched flexure samples, respectively. Nanowire synthesis on dry fabric is described in the following section.

ZnO nanowire synthesis on dry fabric

ZnO nanowires have very strong interaction with carbon fibers, as previous studies have suggested [28]. Functional groups, e.g. hydroxyl, carbonyl, and carboxylic

acid, have been found in carbon fibers that create a strong chemical bonding with ZnO [29–31]. ZnO nanowires added at the mid-plane of the laminate were synthesized using a hydrothermal method, in which a ZnO nanoparticle seed layer was deposited on a woven carbon-fiber surface by dip coating [32]. ZnO nanoparticles were formed by mixing solutions of zinc acetate dihydrate and ethanol with sodium hydroxide and ethanol in a volume ratio of 18:7 at 55°C [33]. Then the carbon fibers were covered with ZnO nanoparticles by dip coating [26]. After that, nanowires were grown in a glass beaker on a hot plate, where the deposition on carbon fibers occurred in an aqueous solution of zinc nitrate hydrate and hexamethylenetetramine. The temperature of the solution was maintained at 90°C for 4 hours. Finally, the carbon-fiber layers were removed from the solution and rinsed with 18.2 MΩ water and dried at 100°C [26]. A low-molecular-weight polyethylenimine (Aldrich, $M_w = 25{,}000$) was added to aid uniform growth of nanowires [34].

The morphology (diameter, length, and orientation) and quality of ZnO nanowires synthesized on carbon fibers can be controlled through a number of parameters: temperature, solution concentration, ZnO nanoparticle size, and growth time. The approximate final geometry of the ZnO nanowires in this study was 50 nm diameter and 500 nm length [26]. Figure 2 shows scanning electron micrographs of the resulting ZnO nanowires grown on the woven fabric at different scales.

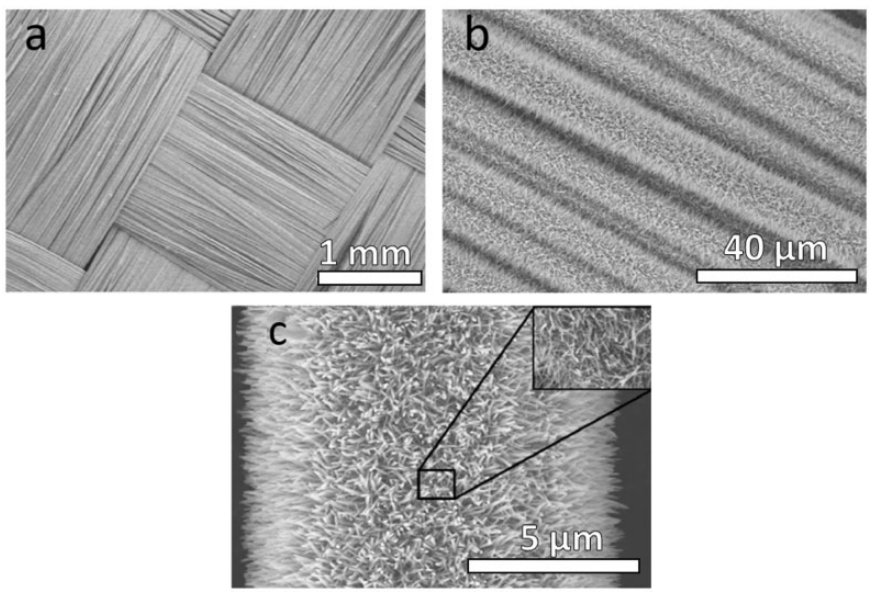

Figure 2. ZnO nanowires grown on 2D woven carbon fiber at different scales: (a) 1 mm, (b) 40 µm, and (c) 5 µm.

Interlaminar fracture toughness

Mode I fracture toughness tests were performed using the double cantilever beam test method. Other possible tests are the wedge-insert-fracture [8] and compression–tension [7] tests. Mode II fracture toughness tests were performed using the end-notched flexure test method. According to Wang and Williams [35], the two common test geometries for Mode II tests are the end-loaded-split and end-notched flexure specimens. The 3-ENF method was originally proposed for testing, but was later developed into the S-ENF, T-ENF and 4-ENF methods [36]. However, according to Pereira et al., [37] the end-notched flexure test is the best method for Mode II testing, owing to its simplicity, negligible friction effects, and low tendency for geometric non-linearity [38].

Mode I fracture toughness: double cantilever beam

Mode I interlaminar fracture toughness, which is the critical strain energy release, measured in joules per square meter, was determined using the double cantilever beam test. The double cantilever beam specimen typically consists of a rectangular uniform-thickness laminated composite with a non-adhesive insert at the mid-plane that serves as a delamination initiator [39]. Opening forces are applied to the double cantilever beam specimen using hinges on the top and bottom surfaces at one end of the specimen by controlling the opening displacement, while the load and delamination length are recorded [39].

Test samples. According to the American Society for Testing and Materials (ASTM) Standard D5528-13, [39] the dimensions (Figure 3) of each specimen were 127 mm (5.0 in) long, 25.4 mm (1.0 in) wide and 2.54 mm (0.1 in) thick. A Teflon sheet of 63.5 mm (2.5 in) length × 25.4 mm (1.0 in) width × 0.05 mm (0.002 in) thickness was inserted to simulate a pre-crack. A pre-crack (about 2 mm) was propagated by loading the hinges with an Instron 8801 machine with a displacement control unit at a loading rate of 5 mm/min (the recommended loading rate was 1–5 mm/min, according to ASTM Standard D5528-13). Eight specimens were tested in total (four specimens with ZnO nanowires and four without ZnO nanowires). The initial

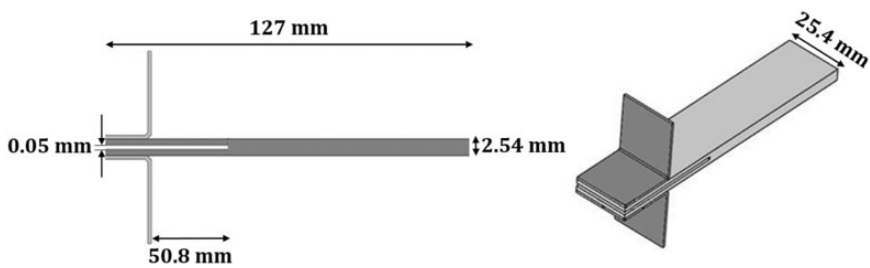

Figure 3. Sample dimensions for double cantilever beam test.

delamination length was measured from the point where the load was applied to the end of the pre-crack. A loading–unloading procedure was followed for crack propagation; the applied displacement was stopped when a significant crack growth accompanied by an abrupt load drop was observed. The crack extension was recorded and the specimens were restored to their original position at an unloading rate of 25 mm/min. About four or five loading–unloading cycles were conducted for each double cantilever beam specimen. All tests were performed in the Manufacturing and Mechanics Laboratory, which is a part of the Challenger-Columbia Structures and Materials Laboratory at the University of Texas at El Paso.

Complex data-reduction methods were used to calculate the critical strain energy release rate, G_{IC}, which is influenced by the accuracy of the measured load, displacement, crack length, and change in compliance with crack length. Three data-reduction methods were applied to the load–displacement data obtained from the tests: (1) modified beam theory, (2) compliance calibration, and (3) modified compliance calibration, as specified in ASTM Standard D5528-13 [39]. Figure 4 shows the double cantilever beam test in progress for one of the specimens.

Mode II fracture toughness: end-notched flexure

Mode II interlaminar fracture toughness, which is the critical strain energy release rate, measured in joules per square meter, was calculated using the end-notched flexure test. The specimen for this test consists of a rectangular, uniform-thickness laminated composite with a non-adhesive insert at the mid-plane that acts as a crack initiator [40]. The end-notched flexure specimen is loaded in a three-point bend fixture that consists of two support points at the bottom and one load point at the top of the specimen at the mid-span [41]. The load, center point displacement, and crack length are measured and recorded during displacement controlled tests.

Figure 4. Double cantilever beam test of carbon-fiber laminate with ZnO nanowires.

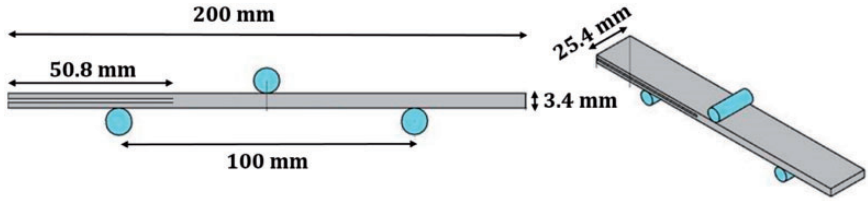

Figure 5. Sample dimensions for end-notched flexure test.

Figure 6. End-notched flexure test of carbon-fiber laminate with ZnO nanowires.

Test samples. According to ASTM Standard D7905/D7905M-14 [40], the dimensions (Figure 5) of each specimen were 200 mm (8.0 in) long, 25.4 mm (1.0 in) wide, and 3.4 mm (0.1 in) thick. A Teflon sheet of 50.8 mm (2.5 in) length × 25.4 mm (1.0 in) width × 0.05 mm (0.002 in) thickness was inserted to simulate a pre-crack. Tests were performed on an Instron 8801 machine at a loading rate of 0.5 mm/min. Eight specimens were tested in total (four specimens with ZnO nanowires and four without ZnO nanowires).

The compliance calibration method is detailed in ASTM Standard D7905 [40] to calculate the Mode II interlaminar fracture toughness value. The specimen was positioned in a three-point bend fixture when the crack length was 30 mm. The specimen was loaded until the crack propagated and an abrupt drop in force was observed. The unloading rate was 0.5 mm/min. The compliance was determined by linear least squares regression analysis of the slope of the load–displacement curve. The fracture toughness was then calculated using the compliance calibration method as described in ASTM Standard D7905. Figure 6 shows the end-notched flexure test in progress for one of the specimens.

Discussion of results

Interlaminar fracture toughness values of composites with and without nanowires were compared, to evaluate the influence of ZnO nanowire reinforcement.

Mode I fracture toughness: double cantilever beam

Mode I fracture toughness (G_{IC}) values of composites with and without nanowires were compared. Figure 7 shows the load–displacement response of one specimen without nanowires. As explained before, the specimen was loaded until an abrupt drop in load was observed. The extent of crack propagation was measured, and

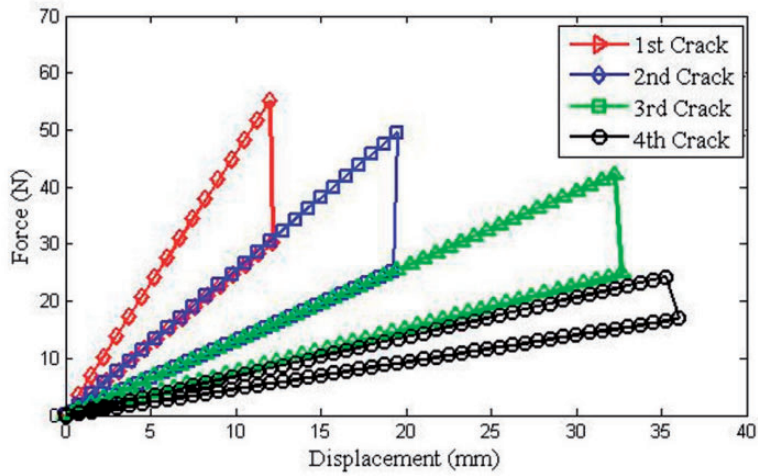

Figure 7. Typical load–displacement response of double cantilever beam test specimen without nanowires.

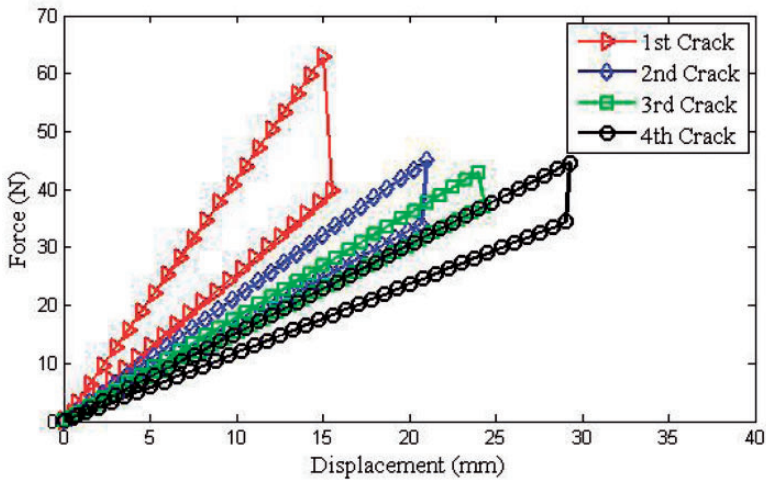

Figure 8. Typical load–displacement response of double cantilever beam test specimen with nanowires.

then the specimen was unloaded to restore it to its original position. This process was repeated until the next load drop occurred. The load–displacement plot for four cycles for a specimen is shown in Figure 7.

Figure 8 shows the load–displacement curve of one of the specimens with ZnO nanowires. The sample without ZnO nanowires (Figure 7) showed larger drops in load corresponding to crack extension. However, the load did not drop as

Table 1. G_{IC} (kJ/m^2) without ZnO nanowires.

Specimen	MBT	CC	MCC
1	0.442	0.414	0.465
2	0.424	0.427	0.477
3	0.424	0.376	0.418
4	0.454	0.505	0.434
Average	0.430 ± 0.001	0.431 ± 0.047	0.449 ± 0.023

CC: compliance calibration; MBT: modified beam theory; MCC; modified compliance calibration.

Table 2. G_{IC} (kJ/m^2) with ZnO nanowires.

Specimen	MBT	CC	MCC
1	0.747	0.772	0.726
2	0.683	0.777	0.734
3	0.718	0.726	0.809
4	0.760	0.914	0.832
Average	0.716 ± 0.026	0.797 ± 0.070	0.775 ± 0.056

CC: compliance calibration; MBT: modified beam theory; MCC: modified compliance calibration.

drastically in the specimen with ZnO nanowires (Figure 8). As stated before, G_{IC} values were calculated using three reduction methods: modified beam theory, compliance calibration, and modified compliance calibration. The values are shown in Tables 1 and 2 for specimens without and with ZnO nanowires, respectively. ZnO nanowire interlaminar reinforcement showed an increase of approximately 66.5% using the modified beam theory method, approximately 84.9% using the compliance calibration method, and approximately 72.6% using modified compliance calibration method. Therefore, ZnO nanowires appear to greatly improve the Mode I interlaminar fracture toughness of carbon woven composites. This increase can be attributed to the bridging effect and cohesive matrix failure of the laminate. An analysis of the surface of a single fiber showed a cohesive matrix failure, which supported resistance of the nanowire toward the formation of new surfaces at the interlaminar regions [26].

Mode II fracture toughness: end-notched flexure

Figures 9 and 10 show the load–displacement response of specimens without and with ZnO nanowire reinforcement for end-notched flexure tests, respectively. The displacements are normalized by the displacement corresponding to

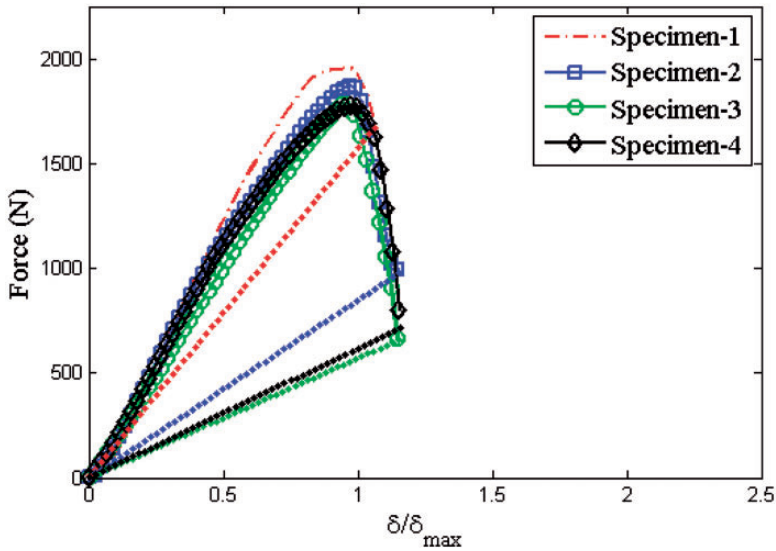

Figure 9. Load–displacement response for specimens without nanowires for end-notched flexure test.

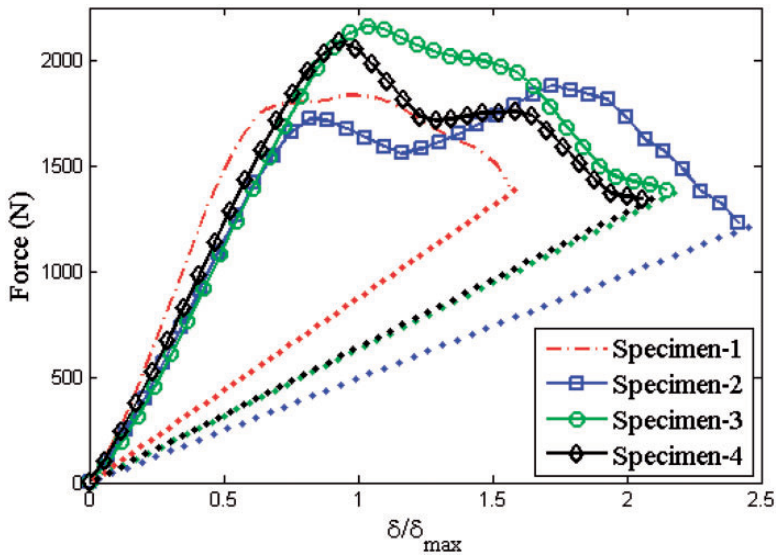

Figure 10. Load–displacement response for specimens with nanowires for end-notched flexure test.

Table 3. G_{IIC} (kJ/m^2).

Specimen	Without ZnO	With ZnO
1	0.422	0.584
2	0.459	0.557
3	0.426	0.513
4	0.437	0.571
Average	0.436 ± 0.014	0.556 ± 0.027

the peak load, to account for the slight increase in thickness due to nanowire reinforcement.

During the experiments, it was noticed that crack progression in the sample without ZnO nanowires was more sudden than that in the samples with ZnO nanowires. This is manifested by a steeper drop in the post-peak response of the samples without ZnO nanowires (Figure 9), as compared with the gradual drop in peak load for samples with ZnO nanowires (Figure 10).

As stated before, G_{IIC} values were calculated using the compliance calibration reduction method; G_{IIC} values calculated for the specimens without and with ZnO nanowires are given in Table 3. ZnO nanowire reinforcement showed an average increase of approximately 28% using the compliance calibration method. This increase is attributed to the shearing effect of ZnO nanowires at the laminate interfaces, thus reducing the ease of creating new smooth fracture surfaces. Therefore, ZnO nanowires appear to improve the Mode II interlaminar fracture toughness of carbon-fiber woven composites.

Fractographic analysis

The fractured surfaces were examined under a scanning electron microscope to explore the interlaminar fracture mechanism of the specimens with and without ZnO nanowires. Fracture surfaces in both cases were restricted in the mid-plane interlaminar region of the composite. In samples without ZnO nanowires, the crack propagated predominantly through the resin, as shown in Figure 11(b). That is, the interface is smooth, with only a small amount of fiber separation at the interface. Whereas, for samples with ZnO nanowires, a large amount of fiber separation at the interface was observed, as shown in Figure 11(a), which is attributed to the ZnO nanowires at the interfaces. Based on these observations, it is hypothesized that the ZnO nanowires improve the bonding between the interfaces. Owing to enhanced shear resistance imparted by the ZnO nanowires, fracture surface progression is accompanied by fiber separation from the layers, which appears to improve the Mode II interlaminar fracture toughness. That is, a higher resistance is present in the sample with ZnO nanowires, where the fracture surface not only propagates through the interlaminar region, but also pulls the carbon fibers, as seen in Figures 11(c) and (d).

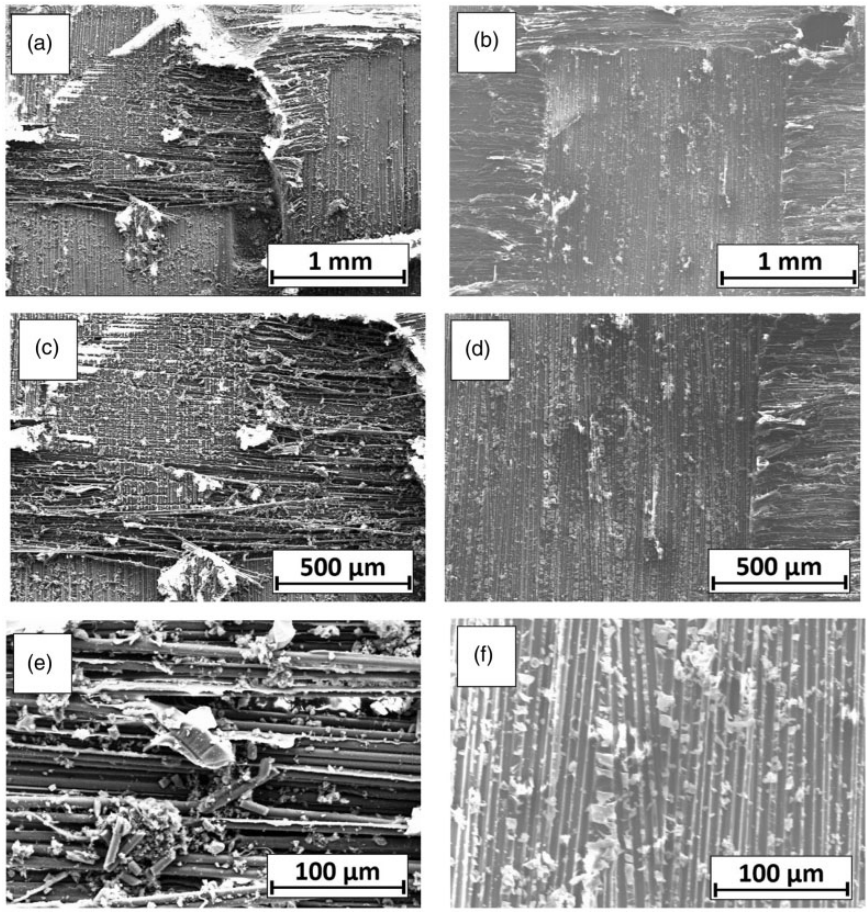

Figure 11. Fracture surfaces for: (a) specimen with ZnO nanowires (scale: 1 mm); (b) specimen without ZnO nanowires (scale: 1 mm); (c) specimen with ZnO nanowires (scale: 500 µm); (d) specimen without ZnO nanowires (scale: 500 µm); (e) specimen with ZnO nanowires (Scale: 100 µm); (f) specimen with ZnO nanowires (Scale: 100 µm).

Conclusions

In this study, Mode I and Mode II interlaminar fracture toughness values of carbon-fiber woven composite face sheets with and without ZnO nanowire reinforcement at the interlaminar regions were compared. Double cantilever beam tests were used to determine Mode I fracture toughness values with three data-reduction methods: modified beam theory, compliance calibration, and modified compliance calibration. End-notched flexure tests were used to determine Mode II fracture toughness values, using the compliance calibration method. Eight specimens were tested for each mode; four with ZnO nanowires and four

without. This study revealed that the Mode I interlaminar fracture toughness increased significantly: approximately 66.5% using modified beam theory, 84.9% using the compliance calibration method and 72.6% using the modified compliance calibration method. The Mode II interlaminar fracture toughness of samples with ZnO nanowires increased by approximately 28%, compared with samples without ZnO nanowires. Therefore, this study shows that very promising results can be obtained by adding ZnO nanowires at the interlaminar regions to improve Mode I and Mode II fracture toughness values.

Acknowledgments

The authors would like to thank Dr. Yapa Rajapakse and Dr. Asher Rubinstein for their support. Further, the authors would like to acknowledge Mr. Sergio Quevedo for his assistance in performing a few preliminary experiments.

Funding

The author(s) disclosed receipt of the following financial support for the research, authorship, and/or publication of this article: This work was supported by the DoD HBCU/MI Basic Research Grant (grant number W911NF-15-1-0430), the University of Texas at El Paso Provost Research Grant, and the Campus Office for Undergraduate Research Initiative at the University of Texas at El Paso.

References

1. Smiley AJ and Pipes RB. Rate effects on Mode I interlaminar fracture toughness in composite materials. *J Compos Mater* 1987; 21: 1–18.
2. Tenney D, Davis J, Byron R, et al. NASA composite materials development: lessons learned and future challenges. In: *NATO RTO AVT-164 Workshop on Support of Composite Systems*, Bonn, Germany, 19–22 October 2009, paper no. LF99-9370, pp.1–58. Neuilly-sur-Seine, France: NATO Research and Technology Organization.
3. Bortz DR, Merino C and Martin-Gullon I. Mechanical characterization of hierarchical carbon fiber/nanofiber composite laminates. *Composites Part A* 2011; 42: 1584–1591.
4. Lars B, Sumfleth J, Hedemann H, et al. Improvement of fatigue life by incorporation of nanoparticles in glass fibre reinforced epoxy. *Composites Part A* 2010; 41: 1419–1424.
5. Galan U, Lin Y, Ehlert GJ, et al. Effect of ZnO nanowire morphology on the interfacial strength of nanowire coated carbon fibers. *Compos Sci Technol* 2011; 71(7): 946–954.
6. Wicks S, Wang W, Williams MR, et al. Multi-scale interlaminar fracture mechanisms in woven composite laminates reinforced with aligned carbon nanotubes. *Compos Sci Technol* 2014; 100: 128–135.
7. Szekrenyes A. Overview on the experimental investigations of the fracture toughness in composite materials. *Hungarian Electronic Journal of Sciences* 2002; MET-020507-A: 1–19.
8. Czabaj M and Ratcliffe J. Comparison of intralaminar and interlaminar Mode-I fracture toughness of unidirectional IM7/8552 graphite/epoxy composite. In: *2012 American Society for Composites*, Arlington, TX, 1–3 October 2012, paper no. NF1676L-15094..
9. Arguelles A, Vina J, Canteli AF, et al. Interlaminar crack initiation and growth rate in a carbon-fibre epoxy composite under Mode I fatigue loading. *Compos Sci Technol* 2008; 68: 2325–2331.

10. Khan R, Rans CD and Benedictus R. Effect of stress ratio on delamination growth behavior in unidirectional carbon/epoxy under Mode I fatigue loading. In: *ICCM-17 International Conferences on Composite Materials*, Edinburgh, Scotland, 27–31 July 2009, pp.1–11.
11. O'Brien K. Characterization of delamination onset and growth in a composite laminate. *NASA Technical Memorandum* 1981; 1–63. ASTM Symp. on Damage in Composite Mater.: Basic Mech., Accumulation, Tolerance, and Characterization; 10–14 November 1980; Bal Harbour, FL; United States.
12. Rikards R, Buchholz FG, Bledzki AK, et al. Mode I, Mode II and Mixed-mode I/II interlaminar fracture toughness of GFRP influenced by fiber surface treatment. *Mech Compos Mater* 1996; 32(5): 1–24.
13. Dransfield KA, Jain KL and Mai YW. On the effects of stitching in CFRPs-I Mode I delamination toughness. *Compos Sci Technol* 1998; 58: 815–827.
14. Prasad MS, Venkatesha C and Jayaraju T. Experimental methods of determining fracture toughness of fiber reinforced polymer composites under various loading conditions. *J Miner Mater Charact Eng* 2011; 10: 1263–1275.
15. Robinson P and Das S. Mode-I DCB testing of composite laminates reinforced with *z*-direction pins: a simple model for the investigation of data reduction strategies. *Eng Fract Mech* 2004; 71: 345–364.
16. Sager RJ, Klein PJ, Davis DC, et al. Interlaminar fracture toughness of woven fabric composite laminates with carbon nanotube/epoxy interleaf films. *J Appl Polym Sci* 2011; 121: 2394–2405.
17. Kong K, Deka BK, Kim M, et al. Interlaminar resistive heating behavior of woven carbon fiber composite laminates modified with ZnO nanorods. *Compos Sci Technol* 2014; 100: 83–91.
18. Fan Z, Santare MH and Advani SG. Interlaminar shear strength of glass fiber reinforced epoxy composites enhanced with multi-walled carbon nanotubes. *Composites Part A* 2008; 39: 540–554.
19. Ashrafi B, Guan J, Mirjalili V, et al. Enhancement of mechanical performance of epoxy/carbon fiber laminate composites using single-walled carbon nanotubes. *Compos Sci Technol* 2011; 71: 1569–1578.
20. Qian H, Bismarck A, Greenhalgh ES, et al. Hierarchical composites reinforced with carbon nanotube grafted fibers: the potential assessed at the single fiber level. *Chem Mater* 2008; 20: 1862–1869.
21. Kong K, Deka BK, Kwak SK, et al. Processing and mechanical characterization of ZnO/polyester woven carbon-fiber composites with different ZnO concentrations. *Composites Part A* 2013; 55: 152–160.
22. Hwang H, Malakooti M, Patterson B, et al. Increased interyarn friction through ZnO nanowire arrays grown on aramid fabric. *Compos Sci Technol* 2014; 107: 75–81.
23. Baxter JB and Eray SA. Nanowire-based dye-sensitized solar cells. *Appl Phys Lett* 2005; 86(5): 053114 1–3.
24. Wang XD, Song JH, Liu J, et al. Direct-current nanogenerator driven by ultrasonic waves. *Science* 2007; 316: 102–105.
25. Wang ZL and Song J. Piezoelectric nanogenerators based on zinc oxide nanowire arrays. *Science* 2006; 312: 242–246.
26. Lin Y, Ehlert G and Sodano H. Increased interface strength in carbon fiber composites through a ZnO nanowire interphase. *Adv Funct Mater* 2009; 19: 2654–2660.

27. Chittajallu K. *Computational modeling of the vacuum assisted resin transfer molding (VARTM) process*. MS Thesis, Clemson University, 2004.
28. Crook S, Dhariwal H and Thornton G. HREELS study of the interaction of formic acid with ZnO(1010) and ZnO(0001)-O. *Surf Sci* 1997; 382(1–3): 19–25.
29. Dilsiz N and Wightman JP. Surface analysis of unsized and sized carbon fibers. *Carbon* 1999; 37(7): 1105–1114.
30. Dilsiz N and Wightman JP. Effect of acid–base properties of unsized and sized carbon fibers on fiber/epoxy matrix adhesion. *Colloids Surf A* 2000; 164: 325–336.
31. Turgeman R, Gershevitz O, Deutsch M, et al. Crystallization of highly oriented ZnO microrods on carboxylic acid-terminated SAMs. *Chem Mater* 2005; 17: 5048–5056.
32. Ehlert GJ. *Development of a zinc oxide nanowire interphase for enhanced structural composites*. PhD Thesis, University of Florida, 2009.
33. Hu Z, Oskam G and Searson P. Influence of solvent on the growth of ZnO nanoparticles. *J Colloid Interface Sci* 2003; 263: 454–460.
34. Law M, Greene LE, Johnson JC, et al. Nanowire dye-sensitized solar cells. *Nat Mater* 2005; 4: 455–459.
35. Wang Y and Williams JG. Corrections for Mode-II fracture toughness specimens of composite materials. *Compos Sci Technol* 1992; 43: 251–256.
36. Yoshihara H. Mode II initiation fracture toughness analysis for wood obtained. *Compos Sci Technol* 2005; 65: 2198–2207.
37. Pereira AB, Morais ABD, Marques AT, et al. Mode II interlaminar fracture of glass/epoxy multidirectional laminates. *Composites Part A* 2004; 35(2): 265–272.
38. Reis PNB, Ferreira JAM, Costa JDM, et al. Interlaminar fracture in woven carbon/epoxy laminates. *Frattura ed Integrita Strutturale* 2014; 30: 431–437.
39. American Society for Testing and Materials International D5528-13. Standard test method for Mode I interlaminar fracture toughness of unidirectional fiber-reinforced polymer matrix composites.
40. American Society for Testing and Materials International D7905/D7905M-14. Standard test method for Mode II interlaminar fracture toughness of unidirectional fiber-reinforced polymer matrix composites.
41. Zhu Y. *Characterization of interlaminar fracture toughness of a carbon/epoxy composite material*. MS Thesis, Pennsylvania State University, USA, 2009.